Qusai. T. Abdulwaha
College of Engineering
University of Basrah
Basrah, Iraq
qusai.talib@gmail.com

Stress Intensity Factor in Hollow Square Sections Using Extended Finite Element Method

Abstract- *Hollow sections are extensively used in structural applications due to its good mechanical properties relative to weight. The presence of cracks in structural member may lead to catastrophic failure under different loading conditions. The presence of central crack in one side under tensile load is studied for different crack sizes (a/w) ranging from 0.1 to 0.٨. The section is then investigated under bending moment for same crack size and geometry. The values of stress intensity factor (K_I) were evaluated using Extended Finite Element Method (XFEM) and found very close between tensile and bending for same crack sizes but there was a difference in the shape factor values. The section is also investigated under tensile load but with the presence of edge crack with range of crack sizes (a/w) from 0.1 to 0.8. The results showed that the stress intensity factor in edge crack is much higher than central crack for same geometry and under same loading condition.*

Received on: 18/01/2017
Accepted on: 17/08/2017

Keywords- *Stress intensity factor, Crack, Hollow sections, Extended Finite Element.*

How to cite this article: Q. T. Abdulwahab ,“ Stress Intensity Factor in Hollow Square Sections Using Extended Finite Element Method,” *Engineering and Technology Journal*, Vol. 36, Part A, No. 2, pp. 196-201, 2018.

1. Introduction

Hollow sections have excellent resistance to loading in compression, torsion and bending in all directions due to its high second moment of area relative to cross sectional area. Being of good looking shape with less sharp corners, good corrosion resistance and high tensile resistance, hollow sections attracted architects to use them in many structural applications. In addition hollow sections are heavily used in civil, mechanical, transport applications…etc.

Because of their structural applications nature, the presence of discontinuities like flaws or through thickness cracks may cause catastrophic failure in structural member and hence the whole structure. Determination of the effect of the discontinuities and defects is necessary yet not an easy task. The determination of stress distribution and Stress Intensity Factor (SIF) in a section with crack is of major importance to all types of engineering applications [1] and hence received considerable amount of research globally. The stress intensity factor (SIF) is an essential parameter in specifying working life of structure with having cracks [2]. The real practice states that SIF is a complicated function that depends on many factors such as load type and orientation, boundary conditions, crack growth, geometry, and material properties. Many numerical techniques and procedures were employed and developed for the determination of SIF. The Finite Element Method (FEM) is widely used method for the determination of SIF [3-5]. Though the FEM method is accurate and well established but unfortunately it suffer from limitation when dealing with subjects like fracture mechanics and crack propagation. To face this problem re-meshing is used to create new meshes continuously as the deformation increased. Re-meshing is time consuming and requires great computation cost. A new approach is introduced called Extended Finite Element Method (XFEM) [6]. In this approach discontinuous enrichment functions are to be inserted to the FEM approximation to account for discontinuities in the structure. This method allows the crack to be arbitrarily aligned within the mesh. A great deal of research work all around the world in different fields showed excellent accuracy of the XFEM in solving two dimensional and three dimensional problems [7,8]. In this study ABAQUS is used to implement XFEM to solve hollow sections with cracks under tensile and bending loading. The use of XFEM under ABAQUS makes it highly accurate in the field of crack simulation [9,10].

2. Rectangular Hallow Section

The section used in this study is a cold formed rectangular carbon steel (Young's Modulus E = 210 GN/m^2 and Poisons ration ν = 0.3) as indicated in Fig. 1. The dimensions are given in

https:// doi.org/10.30684/etj.36.2A.11

2412-0758/University of Technology-Iraq, Baghdad, Iraq

Table 1 and other shape properties and density per unit length of this section are given in Table 2 according to British Standard (BS-EN 10219) [11]

Table: 1 Dimensions and of square hollow sections [11]

Side Length (mm)	Thickness (mm)	Ext-corner Radii (mm)	Int-corner Radii (mm)
120	6	9	6

Table 2: Section Properties and density per unit length [11]

Mass Kg/m	Area (cm^2)	Second Moment (cm^4)
21.2	27	579

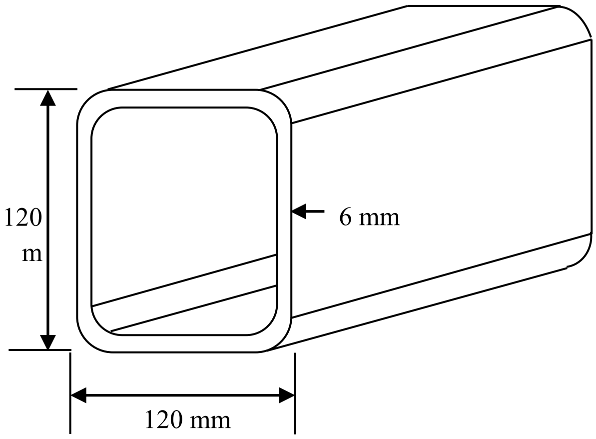

Figure. 1: 120 x 120 hollow square section

I. Stress Intensity Factors

For two dimensional isotropic applications the stress distribution near crack tip may be given by [12] according to linear elastic fracture theory:

$$\sigma_{yy} = \sigma_{xx} = \frac{K_I}{\sqrt{2\pi r}} cos\frac{\theta}{2}\left(1 + sin\frac{\theta}{2} sin\frac{3\theta}{2}\right) \quad (1)$$

where r is distance measured from crack tip and θ represents the orientation. If the stress distribution is required in crack plane then θ is set equal to zero and equation 1 is reduced to:

$$\sigma_{yy} = \sigma_{xx} = \frac{K_I}{\sqrt{2\pi r}} \quad (2)$$

Equation (2) is valid only near crack tip, in this case the distance (r) is only factor that affect the stress distribution.

II. XFEM Approximation

For the current linear elastic fracture mechanics case, let $\Omega \in \mathbb{R}^d$ be continuous domain of d dimensions and $\Gamma_c \in \mathbb{R}^d$ is 2-D crack surface. The extended finite element approximation is given by [6]

$$u(x) = \underbrace{\sum_{i\in k} N_i(x)\, u_i}_{\text{Classical}} + \underbrace{\sum_{i\in k^*} N_i^*(x)\, a_i}_{\text{Discontinuous Enrichment}} + \underbrace{\sum_{i\in k^{**}} N_i^{**}(x)\, b_i}_{\text{Tip Enrichment}} \quad (٣)$$

Where *u(x)* is the total displacement, N_i is classical finite element shape function, N^* is discontinuous enrichment shape function, N^{**} is crack tip enrichment shape function, a_i is displacement due to discontinuous displacement, and b_i is displacement due to the crack tip enrichment. K, K^*, and K^{**} are nodes sets.

The first term is a classical FEM approximation with shape functions $N_i(x)$ and nodal variables u_i. The second term is an enrichment function that takes the discontinuity in the displacement across crack surface into account. The third term or function is an enrichment that accounts for the singular stress strain at crack tip. These two enrichment functions are calculated at nods K^* and K^{**} respectively, see Fig. 2. Additional degrees of freedom are introduced to these nodes namely a_i and b_i.

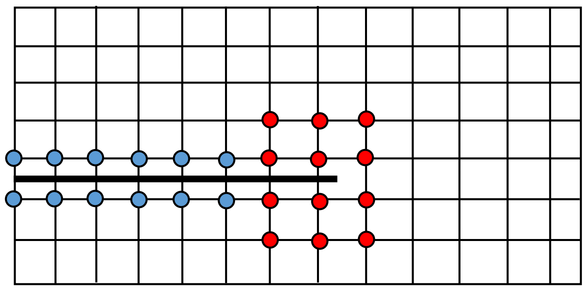

Figure. 2: Definition of the node sets K^* and K^{**}. The nodes in K^* are represented by blue circles and the nodes in K^{**} are represented by red circles

3. Case Studies

In the present research three cases are going to be studies. In the first two cases the loading is going to be axial, while in the third case study bending moment is applied.

I. Square Section with Central Crack Subjected to Axial Load.

In this case a central crack is introduced at the top side of the square section with the load is applied axially (perpendicular to crack plane) as indicated in Fig. 3. In this case the ratio (a/w) is increased from 0.1 mm to 100 mm. The stress intensity factor KI is calculated for each crack length under same loading condition. The results are presented in Fig. 4 shows that in general the increase in crack

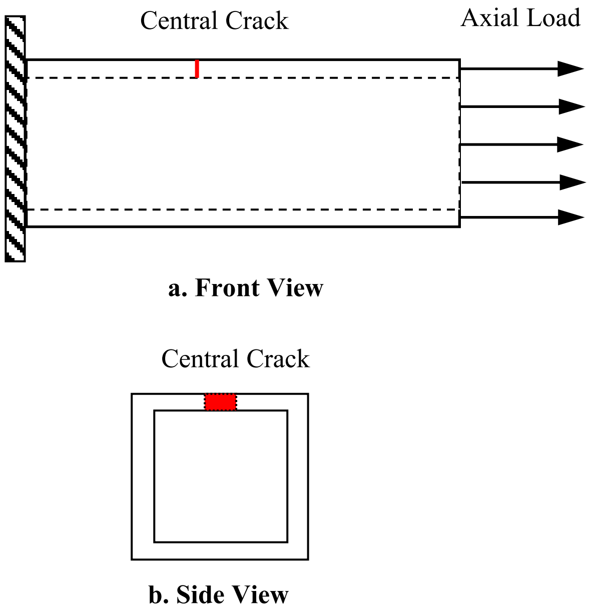

Figure. 3: Front and side view of square section with central crack at top side subjected to axial load

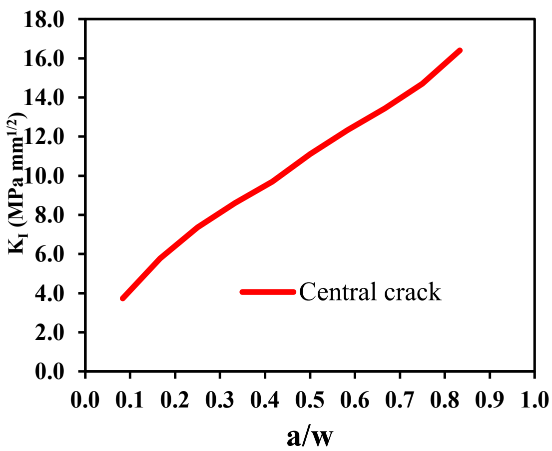

Figure. 4: Relation between central crack length to width of hollow section and stress intensity factor K_I.

leads to proportional increment in the value of stress intensity factor K_I. The shape factor ($C = K_I/K_o$) indicates the effect of the geometry on the level of stress intensity factor is presented in Fig. 5. The correlation factor R is also indicated in Fig. 5 and found to be very strong. The trend of shape factor is increasing as the crack length is increased. The trend of the shape factor as a function of (a/w) is calculated by curve fitting as:

$$C = 1.123(a/w)^3 - 1.560(a/w)^2 + 0.914(a/w) + 0.612 \quad (4)$$

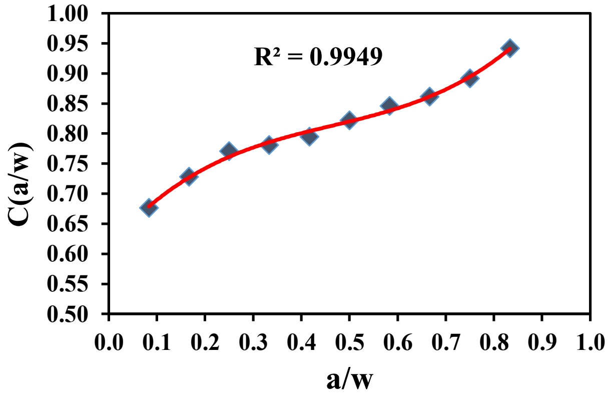

Figure. 5: Relation between central crack length to the width of hollow section and shape factor ($C(a/w) = K_I/K_o$).

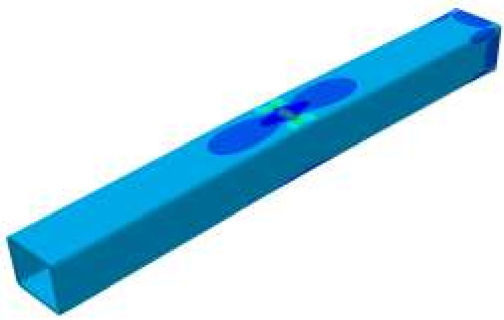

Figure. 6: Stress distribution fringes for (a/w =0.6) central crack

II. Square Section with Edge Crack Subjected to Axial Load.

In this case it is aimed to study the effect of presence of edge crack in one of the corners of the section while being subjected to tensile load. Presence of such crack might affect two sides of the square section and could be thought of presence of two edge cracks in same place at two adjacent sides as shown in Fig. 7.

The stress intensity factor as a function of crack length is presented in Fig. 8 is increasing non-linearly with the length of the crack it rapidly increasing when the crack length to side width (a/w) is 0.6 and more. The levels of KI are clearly much higher than those of central crack in the first case. The reason is that edge crack is in general has higher levels of stress intensity factor than central crack; moreover in the present case the edge crack is presented in two sides of the section which may result in much higher values of K_I.

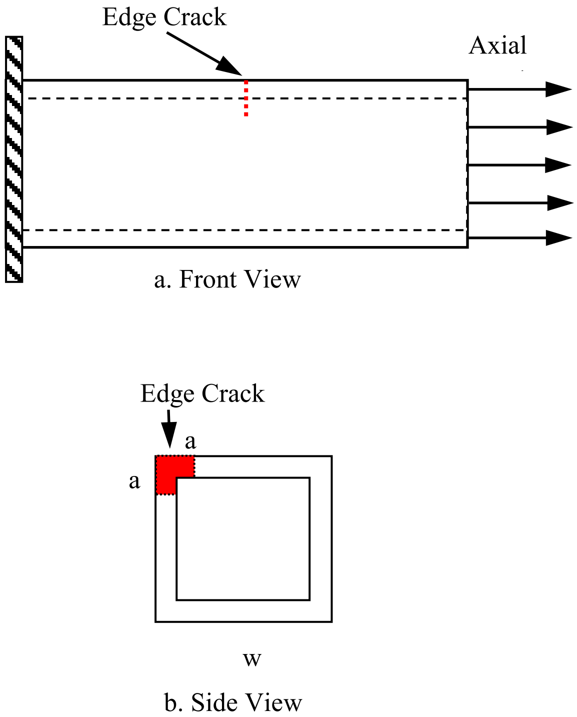

Figure. 7: Front and side view of square section with edge crack at two adjacent sides subjected to axial load

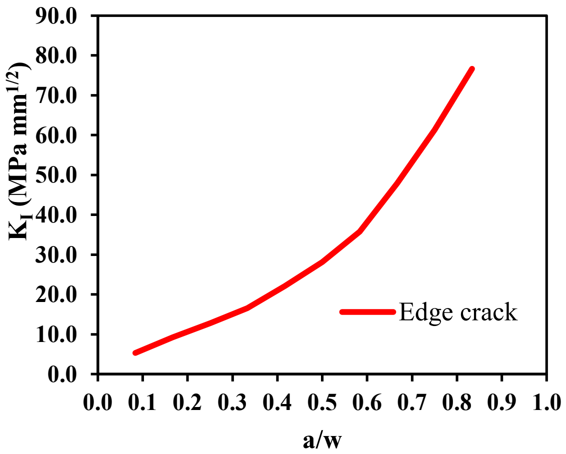

Figure. 8: Relation between edge crack length to width of hollow section and stress intensity factor K_I

The shape factor is presented in Fig. 9 as a function of the ratio of crack length to the width of square section side. The shape factor is also increasing non-linearly as crack size increases. Equation (5) describes the behavior of the shape factor as a function of crack length. It is obvious that the trend of the function in Eq. (6) is of third degree, so that is is increasing rapidly with the increment of crack length.

$$C = 4.991(a/w)^3 - 1.383(a/w)^2 + 1.926a/w + 0.828 \qquad (5)$$

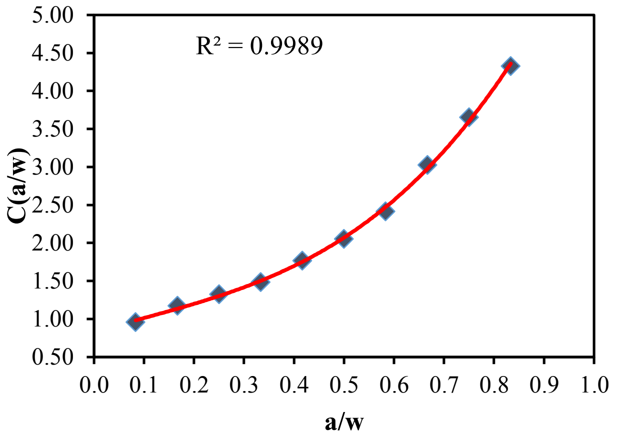

Figure. 9: Relation between edge crack length to the width of hollow section and shape factor ($C(a/w) = K_I/K_o$).

Stress distribution fringes are presented in Fig. 10. The stress at crack tip is very high in the direction of load application. The second principle stress is acting perpendicular to load direction as compression. As a result contraction in crack plane is noted. This contraction might be thought of as buckling. This buckling occurs because the thickness of the section is relatively small that could not withstand second principle stress.

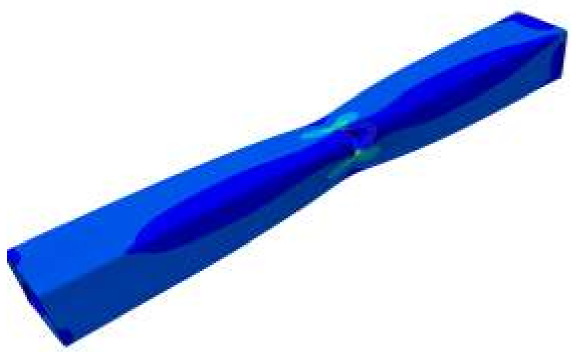

Figure. 10: Stress distribution fringes for (a/w =0.6) edge crack

III. Square Section with Central Crack Subjected to Bending Moment:

Hollow square sections are widely being used in steel structures, so that they are subjected to different loading conditions. One of the most common loading conditions is the bending moment. In this case a square section with central crack (from 10 to 90 mm) see Fig. 11 is subjected to bending moment to investigate the stress intensity factor for this condition.

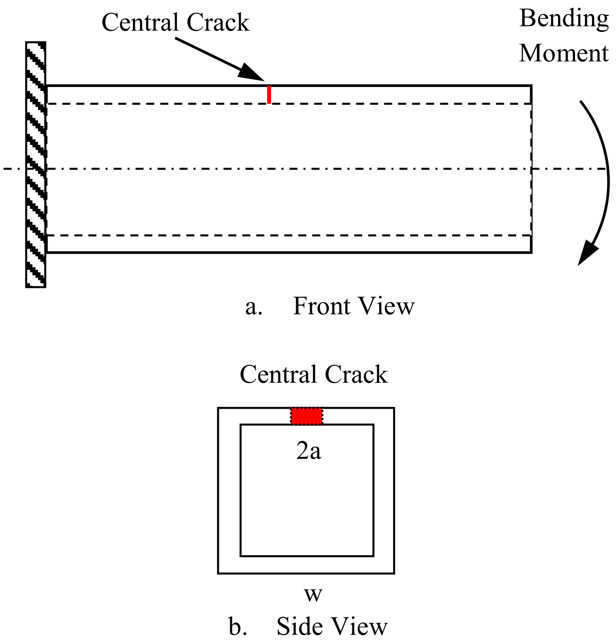

Figure. 11: Front and side view of square section with central crack at top side subjected to bending moment

The stress intensity factor as a function of crack length is presented in Fig. 12 and the shape factor C as a function of crack length divided by side width of hollow square section is given in Fig. 13. It is clear from these two figures that the levels of stress intensity factors are approximately the same as those obtained from tensile. The relation between shape factor and crack length is given in Eq. (6).

$$C = 1.116(a/w)^3 - 1.524(a/w)^2 + 0.871(a/w) + 0.603 \quad (6)$$

K_o in figure 13 for bending moment is given in Eq. (7)

$$K_o = \frac{6M}{w^2}\sqrt{\pi a} \quad (7)$$

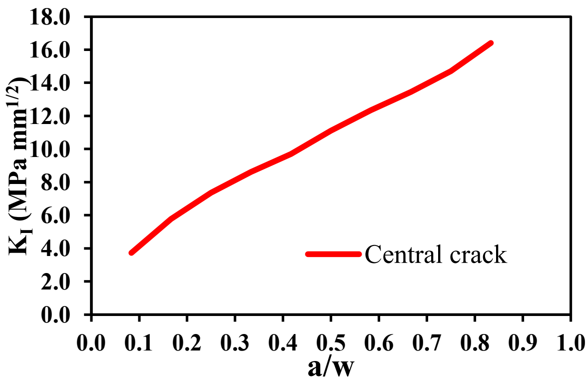

Figure. 12: Relation between central crack length to width of hollow section and stress intensity factor K_I.

The stress distribution fringes are shown in Fig. 14, the maximum stress occurred at crack tips. The stresses on the side of the square section are distributed as tension and compression, while in the middle the stress is much less which indicates the presence of a neutral plane.

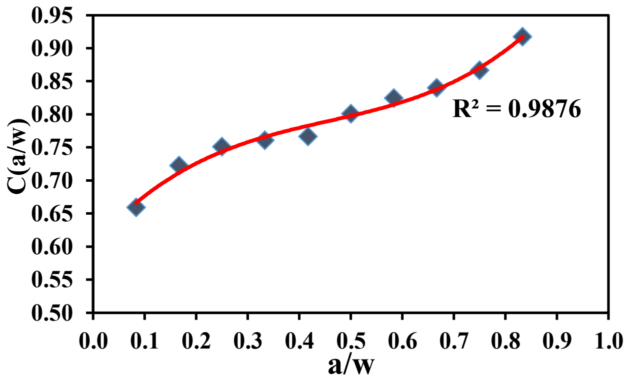

Figure. 13: Relation between central crack length to the width of hollow section and shape factor ($C(a/w) = K_I/K_o$).factor.

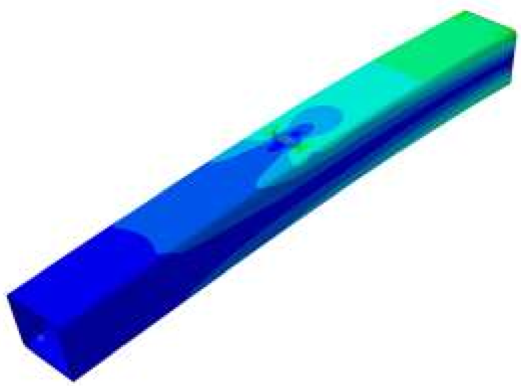

Figure. 14: Stress distribution fringes for (a/w =0.6) edge crack

4. Conclusions:

The obtained results in this study showed that the presence of crack in a hollow section member may result to a very high level of stress concentration at crack tip areas. In the case of central crack under tensile and bending moment the results showed that KI is proportional to crack length and it reached relatively high values as much as 18 MPa. mm1/2. The reason that tensile and bending moment loading result in same level of stress intensity factors is that bending moment results in tensile. The difference is that bending moment causes tension and compression in the side of the section. The edge crack caused much higher stress concentration and stress distribution. It is obvious edge crack is more dangerous than central crack in hollow sections. The stress intensity factor in the case of edge crack is much higher than those obtained in central crack.

References

[1] L. Zhou and Y. Huang "The Sif Formulae For Some Center Cracked Thin-Walled Members," Fourth Int. Conference on Advances in Steel Structures, Vol. II, China, 2005.

[2] E. Hedayati and M. Vahedi "Using Extended Finite Element Method for Computation of the Stress Intensity Factor, Crack Growth Simulation and Predicting Fatigue Crack Growth in a Slant-Cracked Plate of 6061-T651 Aluminum," World Journal of Mechanics, Vol. 4, No. 1, January, 2014.

[3] D. Stamenkovic, "Determination of Fracture Mechanics Parameters using FEM and J-Integral Approach," Proceedings of the 2nd WSEAS Int. Conference on Applied and Theoretical Mechanics, Venice, Italy, November 20-22, 2006.

[4] A. Abdulnaser, and A. A. Kamal, "Finite element simulation of stress intensity factors in elastic-plastic crack growth," Journal of Zhejiang University SCIENCE A, ISSN 1009-3095 (Print); ISSN 1862-1775 (Online), Volume 7, No. 8, 2006.

[5] M. Souiyah et. al, "Finite Element Analysis of the Crack Propagation of Solid Materials," American Journal of Applied Sciences Vol. 6, No. 7, 2009.

[6] T. Belytschko and T. Black, "Elastic Crack Growth in Finite Elements with Minimal Remeshing," International Journal for Numerical Methods in Engineering", Vol.45 No.5, pp. 601– 620, June, 1999.

[7] M. Baydoun and T. P. Fries, "Crack Propagation Criteria in Three Dimensions Using the XFEM and an Explicit–Implicit Crack Description," International Journal of Fracture, Vol. 178, Issue 1, P (51-70), Springer link, 2012.

[8] C. Fan, X. and Q. Jing, "Numerical Study of Crack Propagation Path in Three-Point Bending Beam Using Extended Finite Element Method," Applied Mechanics and Materials, Vols. 353-356, pp. 3615-3618, 2013

[9] E. Giner, N. Sukumer, J.E. Tarancon and F.J. Fuenmayor, "An Abaqus Implementation Of The Extended Finite Element Method," Engineering Fracture Mechanics, Vol.76, pp. 347–368, 2009.

[10] M. McNary, MSc. Thesis, "Implementation of the Extended Finite Element Method (XFEM) In The Abaqus Software Package," Georgia Institute of Technology, Georgia, USA, 2009.

[11] British Standard BS-EN 10219, "Cold formed welded structural hollow sections of non-alloy and fine grain steels. Tolerances, dimensions and sectional properties," 2006.

[12] Ewalds, H. L., Wanhill, R. J. H., "Fracture Mechanics" Edward Arnold, University of Michigan, pp. 15, 1983.

[13] H. I. Khalaf, "Crack Propagation in Plane Stress Problems by Using Experimental and Extended Finite Element Method XFEM," Ph.D. Thesis, Mechanical engineering Department, University of Basrah, Basrah, Iraq, 2015.